Turkish Journal of Electrical Engineering & Computer Sciences

http://journals.tubitak.gov.tr/elektrik/

Research Article

Turk J Elec Eng & Comp Sci
(2017) 25: 4033 – 4049

doi:10.3906/elk-1609-74

A new proposal for the design of hybrid AC/DC microgrids toward high power quality

Pouria GOHARSHENASAN KHORASANI, Mahmood JOORABIAN*, Seyed Ghodratolah SEIFOSSADAT
Department of Electric Power Engineering, Faculty of Engineering, Shahid Chamran University, Ahvaz, Iran

Received: 08.09.2016 • **Accepted/Published Online:** 09.03.2017 • **Final Version:** 05.10.2017

Abstract: Considering the advantages of DC microgrids, the extension of the conventional AC distribution grid can be implemented using a DC microgrid. This justifies the realization of a hybrid AC/DC microgrid. In the present study, a new global solution is presented to improve the power quality and to fully compensate the reactive power of an AC microgrid using DC bus capacity while introducing a new design for a hybrid AC/DC microgrid. In the new design, back-to-back connections of two series and parallel converters, as well as the presentation of new controllers and simultaneous utilization of an earthing switch, are proposed. The proposed method guarantees the quality of the delivered voltage to consumers and the drawn current from the network according to the IEEE-519 and IEEE-1159 standards under different power quality problems (e.g., interruptions, sags, harmonics, and any variation in voltage/current signals from pure sinusoidal). Through the proposed design of the new hybrid AC/DC microgrid, as a new feature, the operation of the network in islanded mode can be achieved in accordance with power quality standards even in the worst load quality conditions. It should be noted that in common hybrid microgrids in islanded mode, the delivered voltage quality is proportional to the quality of the consumer's load current. Another possibility of the proposed design is the instantaneous VAR compensation of nonlinear and induction loads of consumers to keep the power factor of the distribution transformer close to unit value. Simulation results indicate that there are acceptable levels of compensation for different types of power quality problems. Total harmonic distortions and total demand distortions are below 3% in both the grid-connected and isolated modes of the hybrid AC/DC microgrid.

Key words: Hybrid AC/DC microgrids, power quality, series-parallel compensation, harmonic compensation, reactive power compensation

1. Introduction

Nowadays, most renewable energy sources (RESs) and distributed generation (DG) units, including photovoltaic (PV) arrays and fuel cells, directly produce DC output power, while other sources like microturbines or wind turbines deliver variable frequency/voltage AC output power. In both modes, the connection of DG to DC systems is usually simpler, more efficient, and more economical. Moreover, to connect energy storage sources (ESSs) and electrical vehicles, there is no need for converters. Many consumers are using modern household appliances and electronic loads fed by a power supply with an AC-to-DC converter, ultimately using DC power. Therefore, a DC environment is a simpler way to more efficiently deliver power to these loads [1–3].

Today there is a global trend to improve electric power systems in smart grids. Although there are

*Correspondence: mjoorabian@scu.ac.ir

different definitions and meanings of "smart grid", there is a general consensus about the characteristics that smart grids must have. According to the EISA 2007 report, the most important characteristics of smart grids are as follows [4]:

- Energy efficiency, sustainability, and RES inputs.
- Reliability, security, ESSs, and DG units (renewable-based).
- Sensing, measurements, and advanced control methods.
- Load usage awareness, real-time energy management system, and advanced load components.
- Integrated information and communication infrastructures complete with cyber security.

Given the advantages of DC microgrids, the above-mentioned features can often be achieved at lower costs with higher efficiency using DC microgrids. Furthermore, given the fact that many AC grids have reached nominal power capacity, there will soon be a need to extend these grids. However, compared to what AC power grids have been designed for, the need to develop the structure of the network is inevitable due to increased energy consumption.

Considering the advantages of DC microgrids, the extension of the conventional AC distribution grid can be implemented using a DC microgrid, indicative of the realization of the hybrid AC/DC microgrid. In this regard, the hybrid AC/DC microgrid is one of the most promising new research projects conducted in the last decade to optimize the performance of smart grids. In this paper, some of the recent studies conducted on hybrid AC/DC microgrids are reviewed. The different structures of the hybrid AC/DC microgrid and its coordination control algorithms were proposed in [5–8]. A real-time energy management algorithm was proposed for hybrid AC/DC microgrids, involving sustainable energy and hybrid energy storage, in [9–11]. The desired operating features of the hybrid microgrid can be added through interlinking converters. To this end, appropriate control schemes are developed to control the interlinking converter [12–16]. The concept of introducing some DC islands interconnected with the AC distribution network using an additional DC power line to collect energy generated by the distributed domestic renewable sources was presented in [17,18]. A new hybrid AC/DC microgrid design based on distribution FACTS devices and that aims to enhance microgrid operation performance, such as stabilization of the bus voltage, reduction of the feeder losses, and improvements to the power factor, has been introduced by several authors [19–21]. Issues concerning the power quality of the AC microgrid, utilization of active filters, dynamic voltage restorers, unified power quality conditioners, and the interface converter between sources and microgrids have been proposed in various studies [22–29]; however, according to recent reviews of hybrid AC/DC microgrids, the lack of research is evident in areas concerning the effects of these microgrids on power quality problems. Moreover, modern electronic loads are more sensitive and require high power quality, and current distribution networks face many problems, including congested lines and overloaded transformers. As a result, using DC microgrid capacity to cover load demands and power quality enhancement may be an effective tool to solve the current problems of distribution grids and to achieve power quality standards. Therefore, in this paper, a new design of hybrid AC/DC microgrids is presented to improve power quality and to fully compensate the reactive power of the AC microgrid in both grid-connected and isolated modes.

2. Hybrid AC/DC microgrid structure

The term "hybrid AC/DC microgrid" conventionally refers to a microgrid that includes a conventional AC distribution system, as illustrated in Figure 1, and an extension DC grid that is connected to the AC system through one or more parallel bidirectional converters, as illustrated in Figure 2 [5–21]. In the present study, a new design for a hybrid AC/DC microgrid is proposed, while the two back-to-back (B2B) series and parallel converters are connected between AC and DC microgrids, as shown in Figure 3. The DC grid is connected to different renewable energy sources and energy storage sources to supply its local loads and to provide a DC power delivery line to attain several benefits. First, each distributed generator does not have to install AC integration equipment to cope with AC integration problems, such as AC conversion and line synchronization. Second, power management algorithms can easily be applied to B2B converters to allow power sharing between DC and AC grids. Finally, the power delivery line can be utilized for power quality improvements in both isolated and grid-connected modes. To be compliant with the importance of power quality in the next generation of smart grids, this paper is especially focused on power quality assurance in any abnormal conditions through the proposed microgrid structure, as well as using DC bus capacity and introducing two new control schemes for both series and parallel controllers.

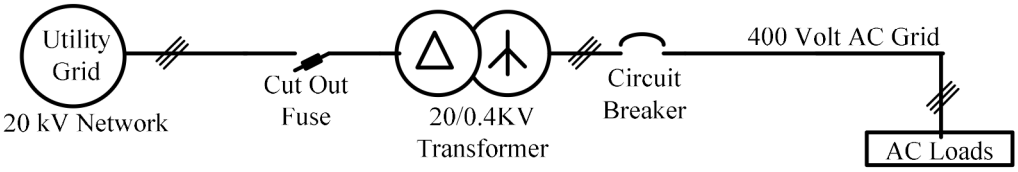

Figure 1. Conventional AC distribution system.

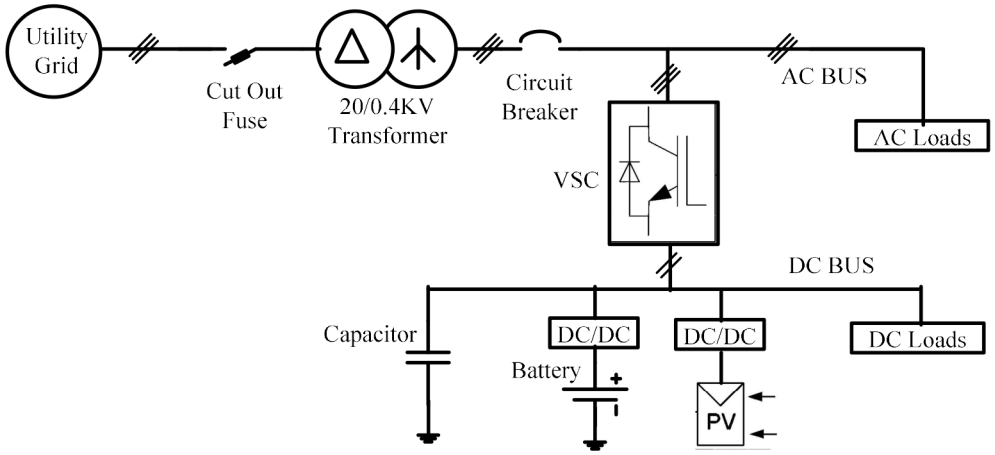

Figure 2. Conventional scheme of the hybrid AC/DC microgrid.

3. Power quality improvement

In the present study, power quality enhancement is summarized in three sections. First, voltage and current quality improvement is described, followed by reactive power compensation, and finally full power quality assurance during the isolated mode of the microgrid is outlined.

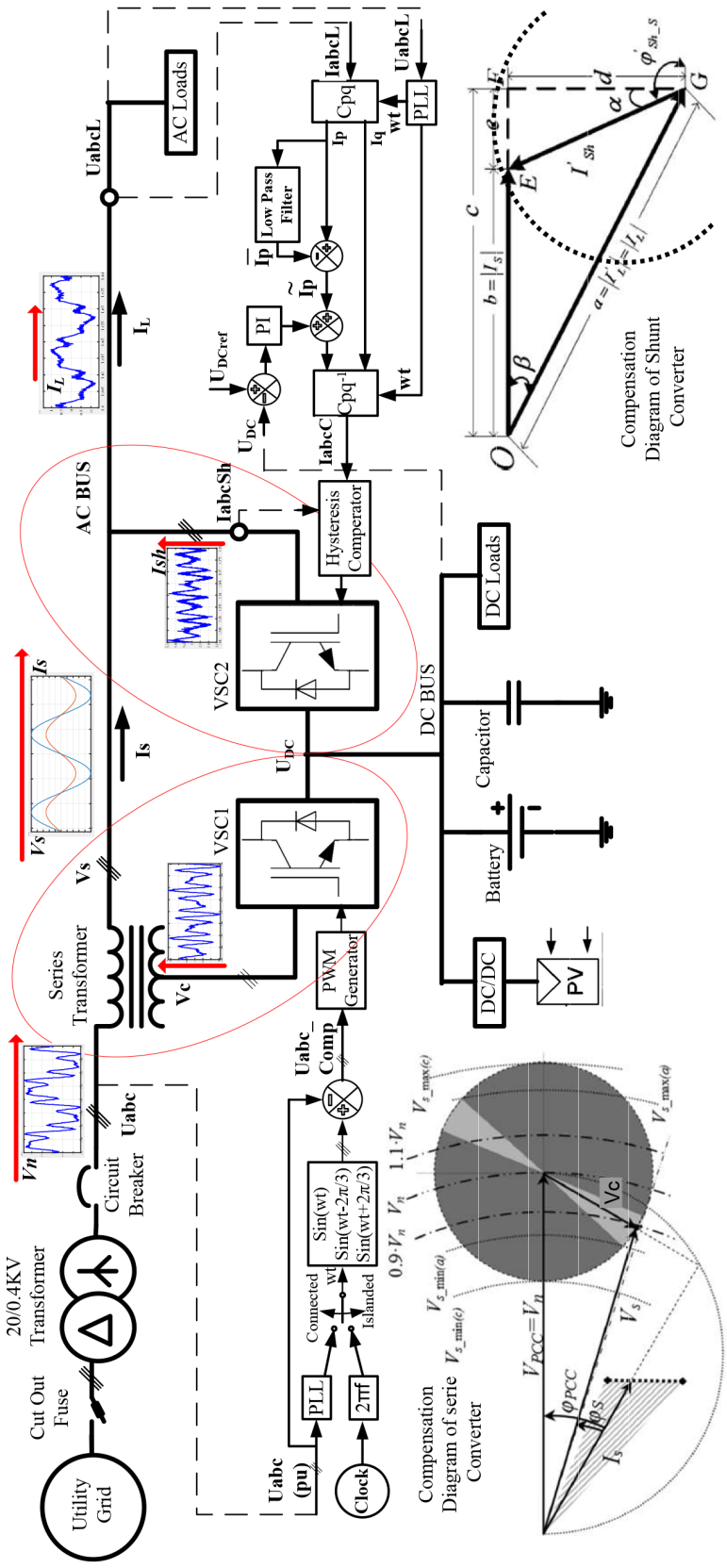

Figure 3. Proposed scheme of the hybrid AC/DC microgrid.

3.1. Voltage and current quality improvement

One of the most important objectives of this study is to exploit a hybrid AC/DC microgrid to keep the total harmonic distortions (THD) of the microgrid voltage and the total demand distortion (TDD) of the microgrid current at less than 5% (according to the IEEE-519 standard) and to keep the voltage variation within $\pm 5\%$ (according to the IEEE-1159 standard) under different power quality issues. Figure 3 is a simple diagram showing series and parallel compensation using two B2B connected voltage source converters. Because of DC bus capacity exploiting and utilizing two degrees of freedom for each converter, compensational diagrams have four-quarter (360°) coverage. Taking this concept into consideration, we try to compensate for the various problems of voltages and currents in this study. It is worth noting that in conventional hybrid AC/DC microgrids, due to the presence of a single voltage source converter, full compensation of the voltage and current at the same time is impossible.

3.2. Reactive power compensation of load

Another potential benefit of the proposed design is the instantaneous VAR compensation of nonlinear and induction loads of consumers to keep the power factor of the distribution transformer close to unit value. In this state, a large portion of the distribution transformer capacity and grid lines will be released. Furthermore, while reducing power distribution losses, the need for normal reactive compensators in the subtransmission substations is also reduced. Figure 4 shows the active and reactive power paths in the proposed scheme. As shown in the figure, the AC microgrid passes only pure active power ($\bar{P}$), while total reactive power (Q) and load disturbances ($\tilde{P}$) are provided by a parallel converter.

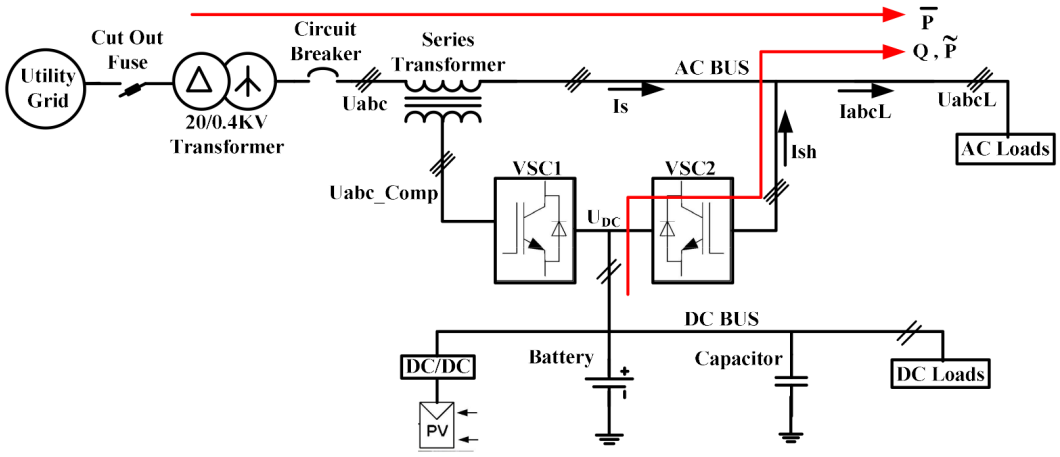

Figure 4. Active and reactive power flow paths of the proposed hybrid AC/DC microgrids.

3.3. Power quality assurance during the islanded mode of the microgrid

When the DC microgrid is appropriately extended and has suitable capacity to generate and store, the hybrid AC/DC microgrid can continue to operate during network interruption in islanded mode. Through the proposed design of the hybrid AC/DC microgrid, the operation of the network in islanded mode can be achieved in accordance with power quality standards, even in the worst load quality conditions. This capability is introduced in this paper for the first time. The key point of the proposed design is that it takes advantage of the series

converter as a static synchronous source. Using an earth switch, the series transformer can deliver the total provided power of the connected converter to the islanded microgrid. The power flow paths are shown in Figure 5a during the islanding mode of the proposed design of the hybrid microgrid. It should be noted that in common hybrid microgrids in islanded mode, the delivered voltage quality is proportional to the quality of the consumer's load current and the quality of the power is not always guaranteed. The power flow path in this mode is shown in Figure 5b.

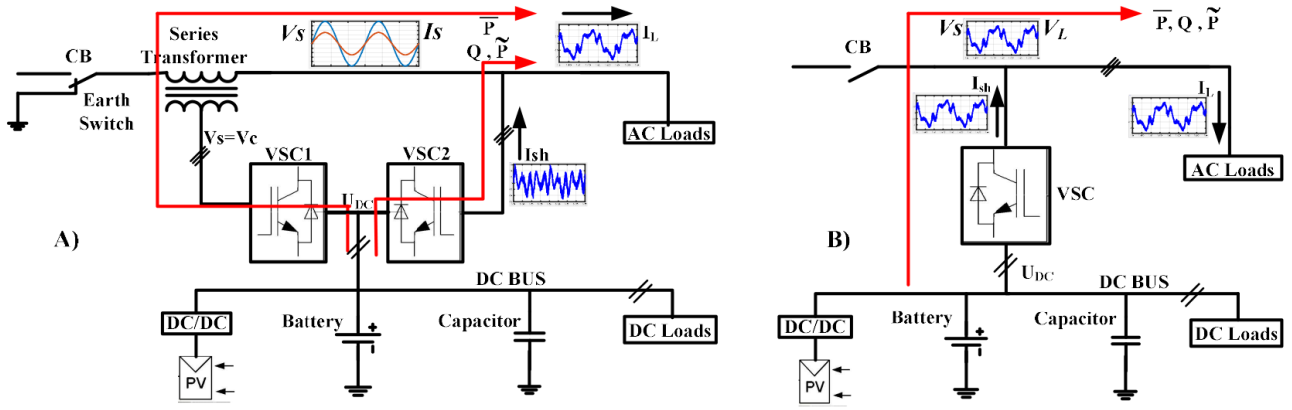

Figure 5. Power flow paths in the hybrid AC/DC microgrid during islanded mode: a) proposed design; b) conventional design.

4. A control scheme to realize the compensational goals

Given the main goal of the present paper in improving both network and consumer power quality using the hybrid AC/DC microgrid potential and with the realization of the goals mentioned in the previous section, the proposed control scheme is introduced for each converter of the hybrid microgrid in this section.

4.1. Parallel compensator control design

The control scheme shown in Figure 6 is proposed to produce the current reference signal for the parallel compensator. This control system is designed in such a way that, in addition to removing all of the power quality problems related to the load current, it also compensates the reactive power under various load conditions, and the voltage level of the DC microgrid is adjusted at the reference value of U_{DCref}.

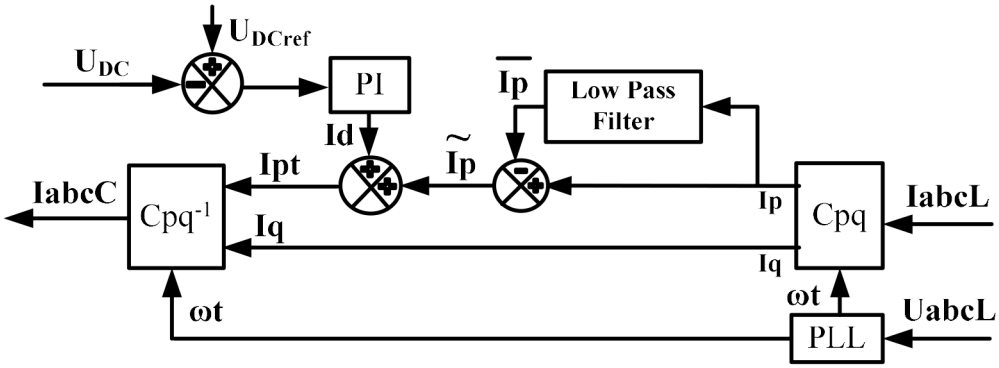

Figure 6. Proposed control design for the parallel compensator.

In Figure 6, UabcL, IabcL, IabcC, U_{DC}, and ωt are the three-phase voltage of load, three-phase current of load, three-phase reference signal for the parallel compensator, DC bus voltage, and angular position of the voltage phasor of UabcL, respectively.

According to the proposed control system (Figure 6), at each sample time, the active and reactive components of the load current (Ip and Iq) are extracted using the Clark transformation (Cpq), based on p-q theory [30], with the phase locked on the load voltage signal via the phase-locked loop (PLL), similar to what is shown in Figure 7. The related equations of the Clark transformation are shown in Eqs. (1)–(3).

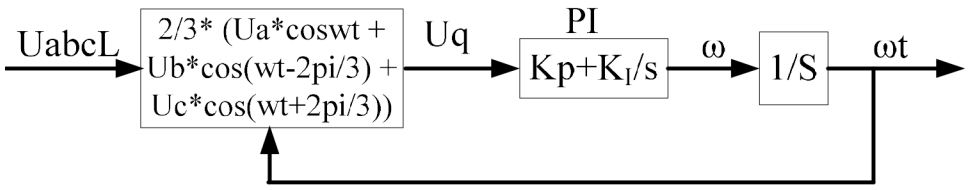

Figure 7. Proposed PLL controller.

$$\mathbf{Ipq} = \mathbf{Cpq} \times \mathbf{IabcL} \tag{1}$$

$$\mathbf{Ipq} = \begin{bmatrix} \mathbf{Ip} & \mathbf{Iq} \end{bmatrix}^{\mathbf{T}} \quad \mathbf{IabcL} = \begin{bmatrix} \mathbf{IaL} & \mathbf{IbL} & \mathbf{IcL} \end{bmatrix}^{\mathbf{T}} \tag{2}$$

$$Cpq = \sqrt{\frac{2}{3}} \begin{bmatrix} Sin\omega t & Sin(\omega t - \frac{2\pi}{3}) & Sin(\omega t + \frac{2\pi}{3}) \\ -Cos\omega t & -Cos(\omega t - \frac{2\pi}{3}) & -Cos(\omega t + \frac{2\pi}{3}) \end{bmatrix} \tag{3}$$

According to the p-q theory, each of the load's current components (active and reactive) includes one average value and one oscillating component. The oscillating component, however, contains all power quality problems. Based on this theory and according to the objective of compensation, each of these values can be selected. In the present study, since parallel compensation involves the compensating of any harmonic distortion and the reactive component of load currents, according to the p-q theory, all reactive components (Iq) and the fluctuating part of the active component ($\tilde{I_P}$) of the load current should be provided by the compensator. As a result, as shown in Figure 6, the average value of the active component ($\bar{I_p}$) is calculated by the low-pass filter, which is then subtracted from the total value ($\mathbf{I_p}$). The result would be the fluctuating value ($\tilde{I_P}$). The related equations are shown in Eqs. (4) and (5), where T_f is the time constant for the low-pass filter.

$$\bar{I_P} = \frac{\mathbf{1}}{\mathbf{1} + \mathbf{T_f} \cdot \mathbf{s}} \mathbf{I_p} \tag{4}$$

$$\tilde{I_P} = I_p - \bar{I_P} \tag{5}$$

Furthermore, to maintain the DC microgrid voltage level, the DC bus voltage error is calculated in relation to the reference value of U_{DCref}. Passing through a PI controller, the active current (Id) amount for injection into or absorption from the DC microgrid can be calculated as Eq. (6) and added to $\tilde{I_P}$ as Eq. (7) to perform the total active component (Ipt) of load current, which must be compensated. Finally, applying an inverse Clark transformation (Cpq^{-1}) on the calculated p-q components (Ipt and Iq), we can extract three-phase reference

currents (IabcC) from the control system, as shown in Eq. (8). These currents will be used as hysteresis reference signals for the inverter. The hysteresis method is used due to its quick response, simple structure for implementation, and low cost.

$$I_d = K_P(U_{DCref} - U_{DC}) + K_I \int (U_{DCref} - U_{DC})dt \tag{6}$$

$$I_{pt} = \tilde{I_P} + I_d \tag{7}$$

$$I_{abcC} = C_{pq}^{-1} \times \begin{bmatrix} Ipt & Iq \end{bmatrix}^T \tag{8}$$

Here, K_P and K_I are the proportional gain and integral gain of the controller, respectively.

4.2. Series compensator control design

The control design shown in Figure 8 is proposed to produce the sinusoid pulse width modulating (SPWM) reference signals for the inverter of the series compensator. In the proposed control scheme, the simplest structure is used to provide both quick response and full compensation of all power quality problems, including interruptions, sags, swells, different phase–voltage asymmetry, and any variation in voltage wave shape from pure sinusoidal.

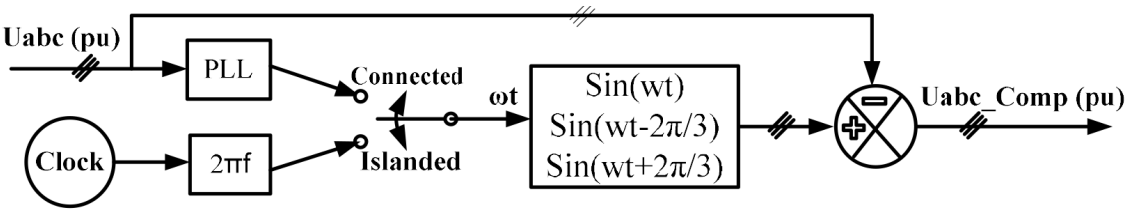

Figure 8. Proposed control scheme for the series compensator.

In Figure 8, Uabc, Uabc_Comp, and ωt are the three-phase voltage of the AC grid, three-phase reference signal for the series compensator, and angular position of the voltage phasor of Uabc or 2πft during isolated mode, respectively. The proposed control system functions in each of the grid-connected and isolated modes as follows.

In the grid-connected mode, the angular position (ωt) of Uabc is extracted via the PLL at any moment, as seen in Figure 7, and is used as the sinusoid function argument. The pu values of the three-phase ideal voltages are calculated, as shown in Eq. (9). The amount of the voltage that should be injected into the grid by the compensator is calculated by comparing the ideal obtained voltages and the instantaneous ones, as shown in Eq. (10).

$$U_{abc\_ideal} = \begin{bmatrix} Sin(\omega t) \\ Sin(\omega t - 2\pi/3) \\ Sin(\omega t + 2\pi/3) \end{bmatrix} \tag{9}$$

$$U_{abc\_Comp} = U_{abc\_ideal} - U_{abc} \tag{10}$$

In the isolated mode, the angular position of the ideal voltage of the AC microgrid is extracted by multiplying the ideal angular velocity of $2\pi f$ by the real time at any moment (clock) and is used as the sinusoid functions

argument. Given the opening of the main circuit breaker of the microgrid in the isolated mode, the value of Uabc is zero. As a result, the ideal obtained voltage is the same amount of voltage that should be injected into the grid by the compensator (Eq. (11)).

$$U_{abc\_Comp} = U_{abc\_ideal} = \begin{bmatrix} Sin(2\pi ft) \\ Sin(2\pi ft - 2\pi/3) \\ Sin(2\pi ft + 2\pi/3) \end{bmatrix} \tag{11}$$

To implement the proposed control system, the SPWM method is used due to its structural simplicity, low cost, and universality. Finally, the compensation voltages (Uabc_Comp) will be used as the SPWM modulating signals for the inverter.

5. Simulation of the hybrid AC/DC microgrid

To study the performance of the proposed design to satisfy the goals mentioned in Section 3, the hybrid AC/DC microgrid shown in Figure 3 is simulated in detail using MATLAB/Simulink, as shown in Figure 9.

5.1. Main grid simulation

As shown in Figure 9, the main AC grid is simulated through a programmable three-phase voltage source, a circuit breaker, series impedance introducing the distribution line, a fault simulator, a set of cut-out fuses, a three-phase 20/0.4-kV transformer with a nominal power capacity of 1 MVA and Dyn11 connection, and a low-voltage circuit breaker. The programmable three-phase voltage source makes it possible to implement a variety of harmonics, amplitude, or phase imbalances and to also represent different sequences (positive, negative, and zero) in the voltage waveforms of the main feeder. The breakers make it possible to isolate the microgrid during any abnormal condition. The fault block provides the possibility of implementation of one-phase, two-phase, or three-phase faults, with or without grounding, using different values of arc and ground resistances.

5.2. Conventional AC grid simulation

As shown in Figure 9, the conventional AC distribution system includes distribution lines and active, reactive, and harmonic loads. For simplicity, all of the loads are located at the end of the distribution line here. Three-phase load power in the symmetrical mode is 600 kW and 200 kVar, and the harmonic loads current includes 150 A of the 2nd harmonic, 500 A of the 5th harmonic, and 200 A of the 7th harmonic.

5.3. DC microgrid simulation

As shown in Figure 9, the DC section of the simulated hybrid AC/DC microgrid consists of several elements such as 700-kW PV arrays controlled with the maximum power point tracking method, a 600-V/500-Ah battery, a 12-F supercapacitor, and, finally, 60 kW of DC loads. In the proposed design, the main sources of energy for the DC microgrid are the PV arrays that provide maximum productive energy of the cells with 600 V of magnitude into the DC network using a boost DC/DC converter. The voltage of the DC microgrid is measured at each moment and is used for the parallel compensator control system (Figure 6) to maintain the DC microgrid voltage level. The presence of the 12-F supercapacitor is very influential in the voltage stability of the DC microgrid, especially during isolation of the hybrid microgrid from the main grid or in the case of fault occurrence in the AC system.

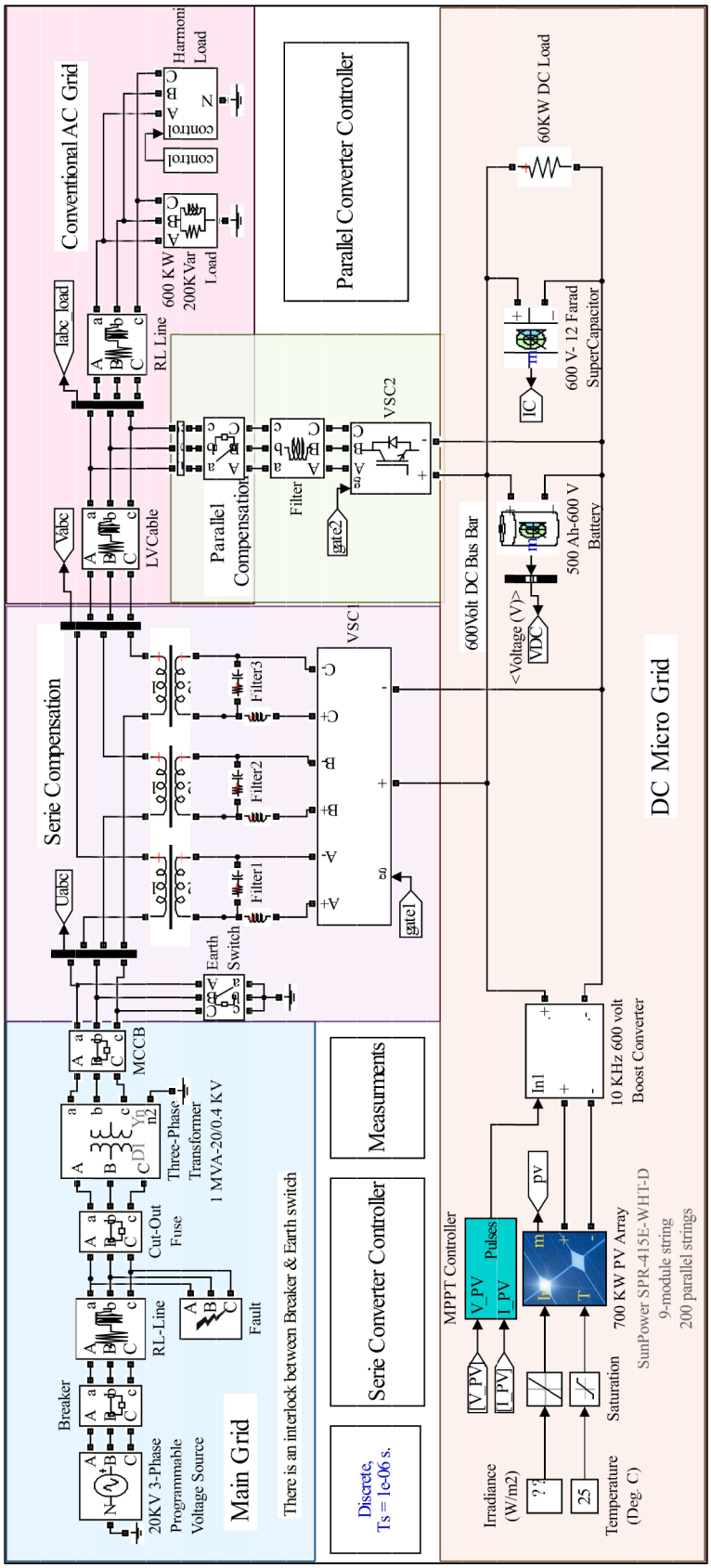

Figure 9. Simulated model of the proposed hybrid AC/DC microgrid in MATLAB/Simulink.

5.4. Series compensator simulation

To simulate the series compensator, three single-phase converters are connected to the grid via three series transformers. These single-phase converters are controlled through pulse width modulation and natural samplings with a frequency of 6 kHz. To reduce noise and high-frequency harmonics, a low-pass filter is used.

Figure 8 shows the design of the controller for this converter. During the connected mode of the hybrid microgrid, the earth switch that has an interlock with a low-voltage molded case circuit breaker is opened and, when the microgrid stands in islanded mode, the earth switch will close.

5.5. Parallel compensator simulation

To simulate the parallel compensator, the three-phase converter is connected to the low-voltage grid via a set of low-pass filters and a three-phase breaker. The three-phase converter is controlled by hysteresis method at a fixed sampling frequency of 10 kHz. The control design for this converter is shown in Figure 6.

6. Simulation results

To evaluate the performance of the proposed schemes toward improving the power quality of the distribution network, different scenarios mentioned in Section 3 are studied and investigated through simulated models in MATLAB/Simulink.

6.1. Compensation results of the load current disturbances

To study the effects of the parallel compensator on improving the current quality (pulled from the AC network), two different states are considered.

The first state includes a balanced three-phase 600-kW active load and a 200-kVar reactive load, along with a harmonic load including 150 A of the 2nd harmonic, 500 A of the 5th harmonic, and 200 A of the 7th harmonic. The current waveform of phase A and of the corresponding harmonic spectrum is shown in Figures 10a and 10b. In this state, the compensated current (pulled from the transformer) and harmonic spectrum are shown in Figures 10c and 10d for the same phase.

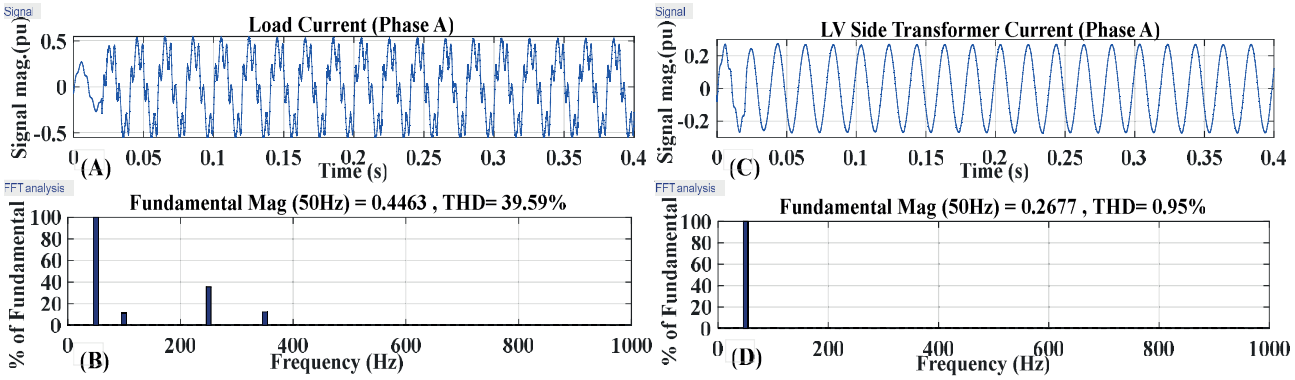

Figure 10. Current waveform of phase A and harmonic spectrum: a, b) load current; c, d) transformer current.

The second state includes the unbalanced three-phase load with load distribution as the first-phase 500-kW active and 200-kVar reactive power, second-phase 300-kW pure active power, and third-phase 400-kW active and 100-kVar reactive power, along with a spectrum of current harmonics (same as in the first state). The current waveform and harmonic spectrum for each phase is shown in Figures 11a–11f. In this state, the

compensated current (pulled from the transformer) and the harmonic spectrum of each phase are shown in Figures 11g–11l.

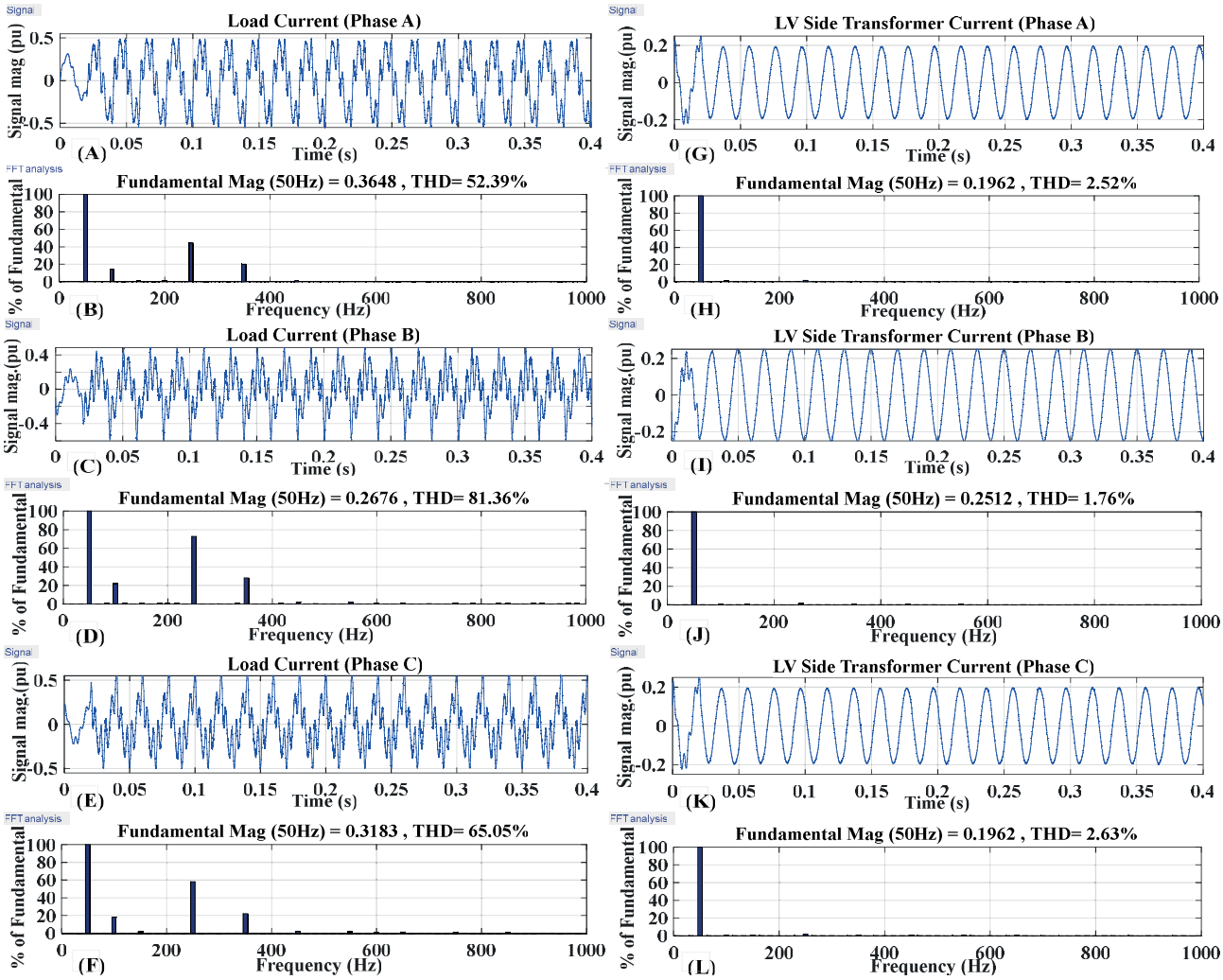

Figure 11. Current waveform and harmonic spectrum: a–f) load current; g–l) transformer current.

As shown in Figure 10, in the grid-connected mode, assuming that grid voltage is standard and when the three-phase load is balanced and contains 39.59% of the TDD after compensation, the TDD of the AC transformer current is limited to 0.95%.

As shown in Figure 11, when the three-phase load is asymmetrical and the magnitude and TDD are 0.36 pu and 52% for the first phase, 0.27 pu and 81% for the second phase, and 0.32 pu and 65% for the third phase, respectively, after compensation, these amounts are limited for the transformer currents to 0.2 pu and 2.52% for the first phase, 0.25 pu and 1.76% for the second phase, and 0.2 pu and 2.63% for the third phase, respectively.

6.2. Compensation results of the reactive current of the load

As mentioned in Section 3, one of the designed control system's objectives is to keep the transformer power factor close to the unit value under different conditions of the load. In this regard, considering two different harmonic loads of balance and unbalance, as mentioned in the previous section, the power factor of the transformer for each state is calculated and shown in Figures 12 and 13.

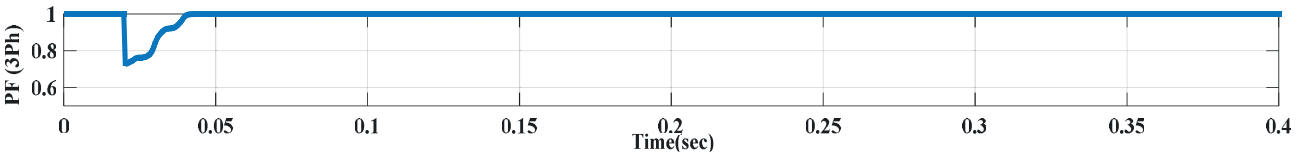

Figure 12. Power factor compensation of balanced load.

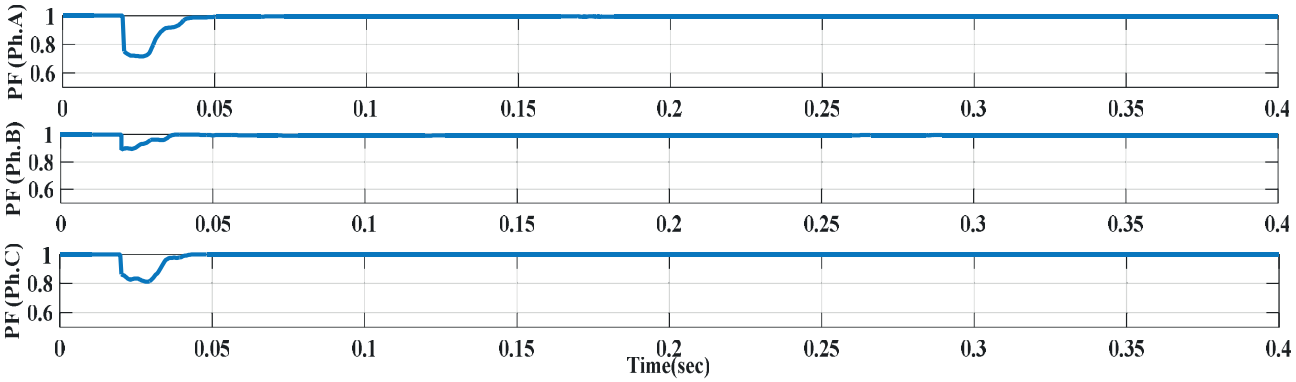

Figure 13. Power factor compensation of unbalanced load.

6.3. Compensation results of the grid voltage disturbances

To study the effects of series compensators on improving the quality of delivered voltage to consumers, the worst network voltage condition is considered as follows. The load's currents are harmonic and asymmetrical, as shown in Figure 11.

The voltage of the AC grid contained 25% of the 5th harmonic and 20% of the 7th harmonic. The steady-state voltage drop (because of line impedance) is 7% and, finally, due to the high impedance fault (phase A to ground via 10 Ω of impedance) in 0.1 s (from 0.15 s to 0.25 s of simulation time), a 33% voltage sag is met. Figures 14a and 14b show the voltage waveform of phase A on the secondary side of the distribution transformer and its harmonic spectrum.

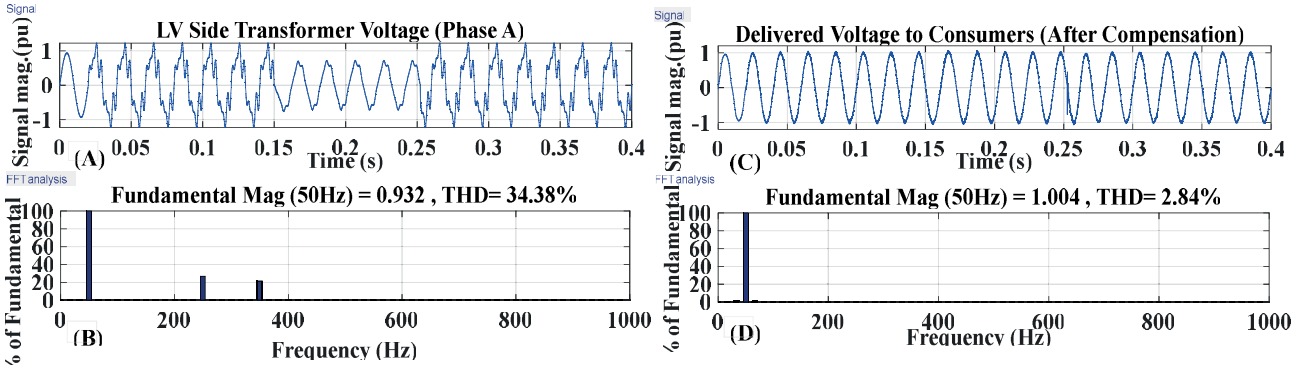

Figure 14. Voltage waveform of phase A and harmonic spectrum: a, b) transformer voltage; c, d) load voltage.

In the case of the presence of the series compensator, the waveform of delivered voltage to consumers and its harmonic spectrum after compensation is shown in Figures 14c and 14d for phase A. Due to space limitations in this paper, showing the other phase's waveform was avoided.

As shown in Figure 14, although the grid voltage contains power quality problems, including 34% of THD, 33% of voltage sag, and 7% of steady-state voltage drop, the delivered voltage to the load is compensated and included only 2.84% of THD and 1 pu of magnitude.

6.4. Power quality assurance results during islanded mode of the microgrid

In this section, as shown in Figure 5a, the circuit breaker is opened, the earth switch is closed, and the hybrid AC/DC microgrid is in islanded mode. However, the load's currents are harmonic and asymmetrical (as shown in Figure 11).

To simulate this scenario, it is assumed that the breaker is opened after 0.1 s of simulation time and the earth switch is closed at the same time. Figure 15 shows three-phase voltages of the AC grid and delivered voltages to the microgrid in this state. The related spectrums of the delivered voltage to the load and drawn current from the series transformer are shown in Figure 16.

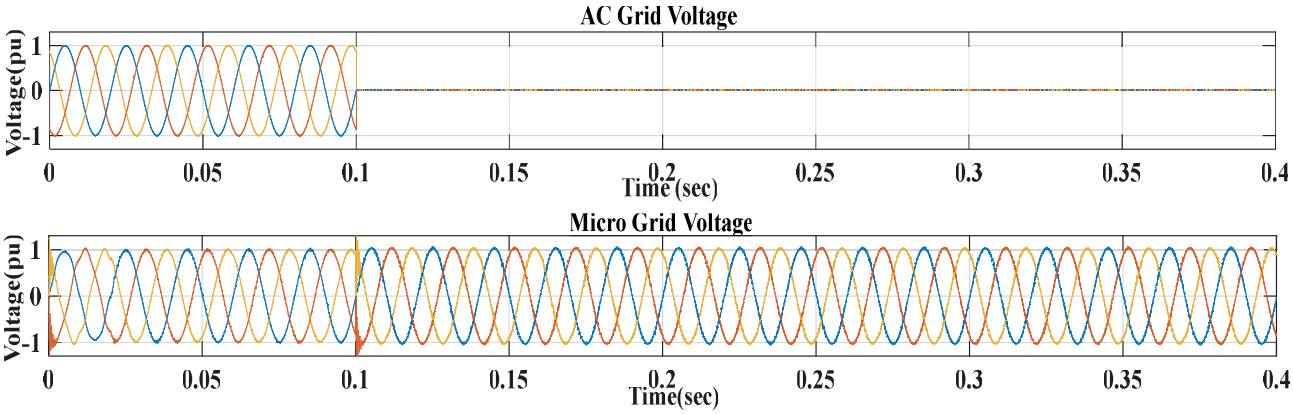

Figure 15. AC grid and microgrid voltage through interruptions.

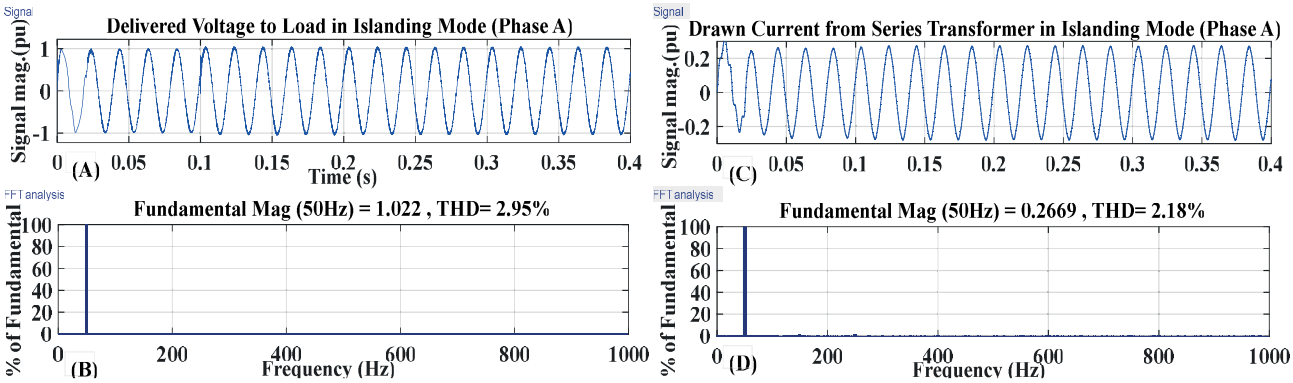

Figure 16. a, b) Voltage of microgrid and related spectrum; c, d) current of series transformer and related spectrum (all in islanded mode).

As shown in Figure 16, although the microgrid is islanded and the load currents are harmonic and asymmetrical (as shown in Figure 11), the delivered voltage to the load and drawn current from the series transformer are compensated for and are relatively pure sinusoid. In conventional hybrid microgrids, the delivered voltage to the microgrid is related to load current quality. To compare how the proposed design and conventional ones are able to face load quality problems in islanding mode, both microgrids are simulated in

similar conditions. Assuming the worst load conditions as shown in Figure 11, the simulation results of the load voltages of two hybrid microgrids (Figure 5) are compared in Figure 17. As shown in this figure, when the load is fed from a conventional hybrid AC/DC microgrid, both the magnitude and THD of the voltage waveforms are affected by load conditions; however, in the proposed design, these delivered waveforms are nearly sinusoidal.

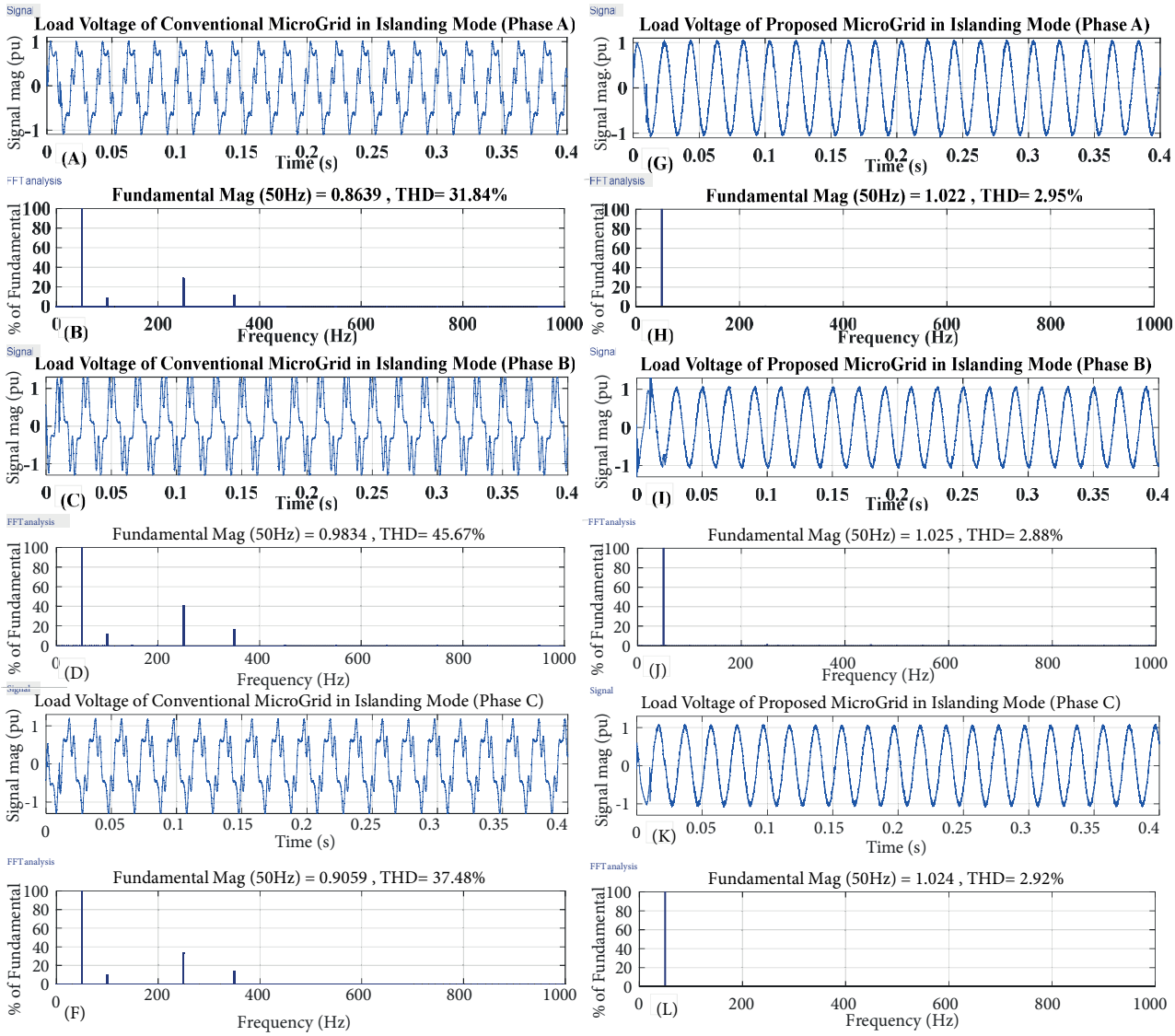

Figure 17. Delivered voltage to the load and related spectrum: a–f) conventional hybrid microgrid; g–l) proposed hybrid microgrid.

6.5. Complexities of simulation to real challenges

Based on the explanation of the control system in Section 4, we can conclude that the proposed system can be implemented with simple standard hardware, namely the ATXMEGA128A1 AVR microcontroller. However, IGBT modules in the medium power range, for example FZ1600R12HP4, can be used as power electronic switches. Another device used in this way is a supercapacitor that is composed of the eight series of the 75-V, 94-F modules, namely the BMOD0094 P075 series from Maxwell Technologies. Subsequently, other devices

in the proposed design can be implemented in reality. In this paper, because of space limitations, only the concept of power quality enhancement is explained, so other challenges, including energy management, power flow control, reliability, stability, and protection of the proposed design of the hybrid AC/DC microgrid, will be discussed in future studies.

7. Conclusion

In this paper, a new proposal was put forward to develop the conventional distribution networks into hybrid AC/DC microgrids through the utilization of the capacity of the DC microgrid and modification of the designs of series and parallel controllers. The simple design of the proposed control systems helps with the fast response and ease of implementation. In the proposed plan, the possibility of simultaneous realization of the goals of power quality and reactive compensation was provided in both the grid-connected and isolated modes of the hybrid microgrid. In summary, realization of the power quality objectives includes maintaining the quality of the voltage delivered to consumers, as well as the currents drawn from the AC grid. As a new feature of the proposed plan, when the hybrid microgrid stands in islanded mode, the series transformers have the role of generating three-phase voltages that are almost sinusoidal. In this case, the power quality of the AC microgrid is guaranteed. Finally, having investigated the results of simulating several scenarios with poor power quality and the need for reactive power compensation, the efficiency of the proposed plan was studied.

Acknowledgment

This work was supported by Shahid Chamran University of Ahvaz.

References

[1] Erdinc O, Uzunoglu M. Optimum design of hybrid renewable energy systems: overview of different approaches. Renew Sust Energ Rev 2012; 16: 1412-1425.

[2] Asmus P. Microgrid, virtual power plants and our distributed energy future. Electricity Journal 2012; 23: 72-82.

[3] Wang P, Goel L, Liu X, Choo FH. A hybrid AC/DC future grid solution. IEEE Power Energy M 2013; 11: 76-83.

[4] Justo JJ, Mwasilu F, Lee J, Jung J. AC-microgrids versus DC-microgrid switch distributed energy resources: a review. Renew Sust Energ Rev 2013; 24: 387-405.

[5] Liu X, Wang P, Chiang L, Loh PA. Hybrid AC/DC microgrid and its coordination control. IEEE T Smart Grid 2011; 2: 278-286.

[6] Lu X, Guerrero JM, Sun K, Vasquez JC, Teodorescu R, Huang L. Hierarchical control of parallel AC-DC converter interfaces for hybrid microgrids. IEEE T Smart Grid 2013; 1: 1-10.

[7] Shaaban MF, Eajal AA, El-Saadany EF. Coordinated charging of plug-in hybrid electric vehicles in smart hybrid AC/DC distribution systems. Renew Energ 2015; 82: 92-99.

[8] Eajal A, Abdelwahed MA, El-Saadany EF, Ponnambalam K. A unified approach to the power flow analysis of AC/DC hybrid microgrids. IEEE T Sust Energ 2016; 7: 1145-1158.

[9] Mohamed A, Salehi V, Mohammed O. Real-time energy management algorithm for mitigation of pulse loads in hybrid microgrids. IEEE T Smart Grid 2012; 3: 1911-1922.

[10] Nejabatkhah F, Lio YW. Overview of power management strategies of hybrid AC/DC microgrid. IEEE T Power Electr 2015; 30: 7072-7089.

[11] Hosseinzadeh FM, Rajaei SF. Power management of an isolated hybrid AC/DC micro-grid with fuzzy control of battery banks. IET Renew Power Gen 2015; 9: 484-493.

[12] Majumder R. A hybrid microgrid with DC connection at back to back converters. IEEE T Smart Grid 2014; 5: 251-259.

[13] Loh PC, Blaabjerg F. Autonomous control of interlinking converter with energy storage in hybrid AC-DC microgrid. IEEE T Ind Appl 2013; 49: 1374-1382.

[14] Shanthi P, Govindarajan U, Parvathyshankar D. Instantaneous power-based current control scheme for VAR compensation in hybrid AC/DC networks for smart grid applications. IET Power Electr 2014; 7: 1216-1226.

[15] Huagen XC, Luo A, Shuai Z, Jin G, Huang Y. An improved control method for multiple bidirectional power converters in hybrid AC/DC microgrid. IEEE T Smart Grid 2016; 7: 340-347.

[16] Peng WE, Jin C, Zhu D, Tang Y, Loh PC, Choo FH. Distributed control for autonomous operation of a three-port AC/DC/DS hybrid microgrid. IEEE T Ind Electron 2015; 62: 1279-1290.

[17] Grillo S, Musolino V, Piegari L, Tironi E, Tornelli C. DC islands in AC smart grids. IEEE T Power Electr 2014; 29: 89-98.

[18] Abdelsalam AA, Gabbar HA, Sharaf AM. Performance enhancement of hybrid AC/DC microgrid based D-FACTS. Int J Elec Power 2014; 63: 382-393.

[19] Karabiber A, Keles C, Kaygusuz A, Alagoz B. An approach for the integration of renewable distributed generation in hybrid DC/AC microgrids. Renew Energ 2013; 52: 251-259.

[20] Mohamed A, Salehi V, Mohammed, O. Reactive power compensation in hybrid AC/DC networks for smart grid applications. In: 3rd IEEE PES Innovative Smart Grid Technologies Europe; 14–17 October 2012; Berlin, Germany. New York, NY, USA: IEEE. pp. 1-6.

[21] Chengshan B, Yang X, Wu Z, Che Y, Guo L, Zhang Sh, Liu Y. A highly integrated and reconfigurable microgrid testbed with hybrid distributed energy sources. IEEE T Smart Grid 2016; 7: 451-459.

[22] Han B, Bae B, Kim H, Baek S. Combined operation of unified power-quality conditioner with distributed generation. IEEE T Power Deliver 2006; 21: 330-338.

[23] Sawant RR, Chandorkar MC. A multifunctional four-leg grid-connected compensator. IEEE T Ind Appl 2009; 45: 249-259.

[24] Wang F, Duarte JL, Hendrix MAM. Grid-interfacing converter systems with enhanced voltage quality for microgrid application–concept and implementation. IEEE T Power Electr 2011; 26: 3501-3513.

[25] Salim RH, Oleskovicz M, Ramos RA. Power quality of distributed generation systems as affected by electromechanical oscillations–definitions and possible solutions. IET Gener Transm Dis 2011; 5: 1114-1123.

[26] Mahdianpoor FM, Hooshmand RA, Ataei M. A new approach to multi-functional dynamic voltage restorer implementation for emergency control in distribution systems. IEEE T Power Deliver 2011; 26: 882-890.

[27] He JW, Li YW, Munir MS. A flexible harmonic control approach through voltage-controlled DG grid interfacing converters. IEEE T Ind Electron 2012; 59: 444-455.

[28] Zin AAM, Naderipour A, Habibuddin MH, Guerrero JM. Harmonic currents compensator GCI at the microgrid. Electron Lett 2016; 52: 1714-1715.

[29] Naderipour A, Zin AAM, Habibuddin MH. Improved power-flow control scheme for a grid-connected microgrid. Electr World 2016; 122: 42-45.

[30] Akagi H, Hirokazu E, Aredes M. Instantaneous Power Theory and Applications to Power Conditioning. 2nd ed. Hoboken, NJ, USA: Wiley-IEEE Press, 2007.